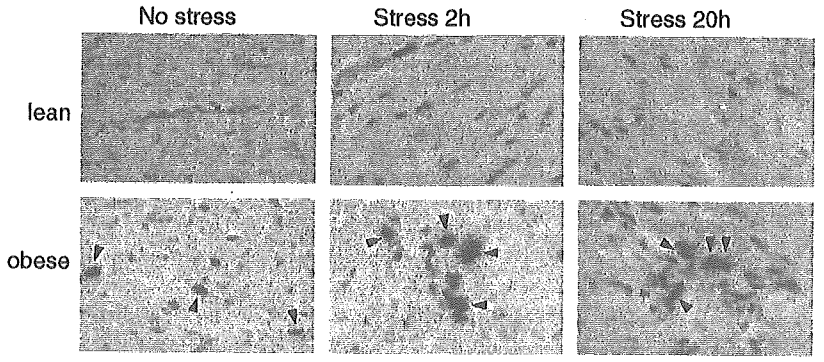

Fig. 3. *In situ* hybridization analysis of PAI-1 mRNA in hearts of the stressed obese and lean mice. Cardiac tissues were harvested from 6-week-old obese and lean mice before and after 2 or 20 h-restraint stress and analyzed by *in situ* hybridization using ^{35}S-labeled cRNA probes as described in Methods. The hybridization signal for PAI-1 mRNA corresponds to black dots in all panels. Arrowheads indicate strongly positive cells for PAI-1 mRNA. All slides were exposed for 12 weeks at 4 °C. Magnification, ×400.

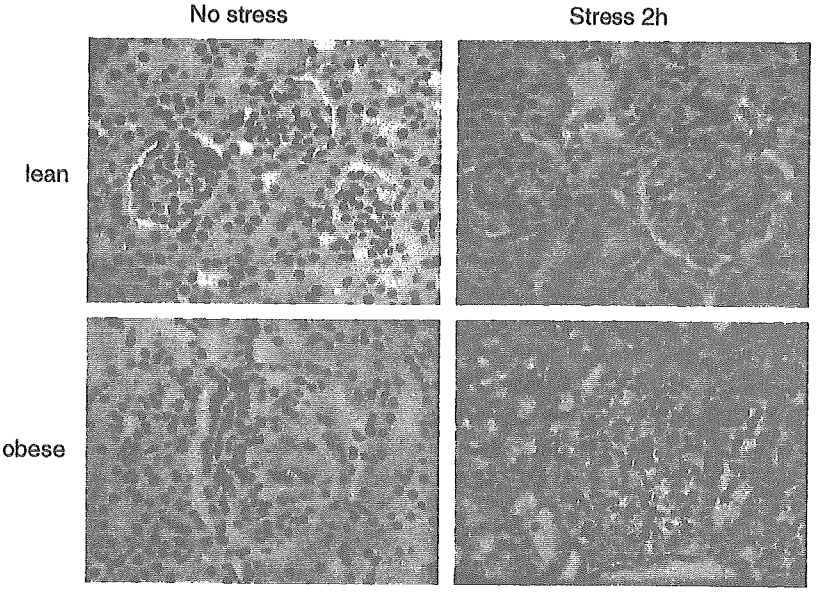

Fig. 4. *In situ* hybridization analysis of PAI-1 mRNA in kidneys of the stressed obese and lean mice. Renal tissues were harvested from 6-week-old obese and lean mice before and after 2 h-restraint stress and analyzed by *in situ* hybridization using ^{35}S-labeled cRNA probes as described in Materials and methods. The hybridization signal for PAI-1 mRNA corresponds to blue dots in all panels. Arrowheads indicate strongly positive cells for PAI-1 mRNA. All slides were exposed for 12 weeks at 4 °C. Magnification, ×400.

Stress-induced fibrin deposition in the kidneys of obese mice

Immunohistochemical analysis of fibrin deposition in renal tissue sections revealed that glomerular fibrin deposition developed after 2 h of restraint stress in obese mice (Fig. 5B), but that no significant glomerular fibrin was detected in stressed lean mice (Fig. 5A). Quantitative analysis of stress-induced fibrin deposition was performed by counting the glomeruli positive for fibrin. Although glomerular fibrin deposition was detected in < 5% of the glomeruli and only in two of eight restraint-stressed lean mice, all of the stressed obese mice (n = 8) showed glomerular fibrin deposition, and the percentages of the glomeruli positive for fibrin in these stressed obese mice were 6–15% (Fig. 5C). Meanwhile, only slight fibrin deposition was observed within the vasculature of the adipose tissue of two of eight stressed obese mice, while none of the stressed lean mice showed fibrin deposition in their adipose tissue (data not shown). No fibrin deposition was detected in other tissues, including the livers, hearts, lungs, and intestines of the obese mice after 2 h-restraint (data not shown).

Discussion

Although obesity and physicopsychological stress are associated with an increased incidence of cardiovascular/thrombotic diseases, little information is available about the underlying

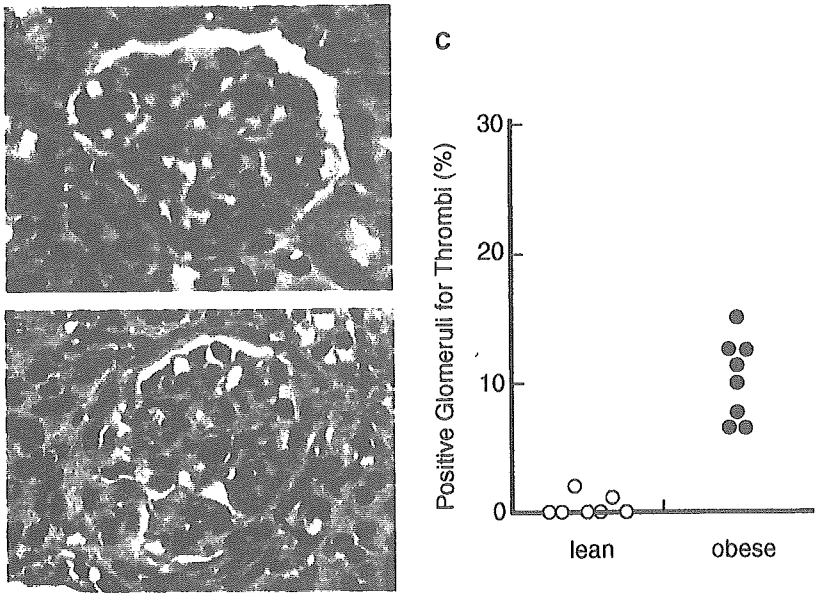

Fig. 5. Stress-induced glomerular fibrin deposition in obese and lean mice. Renal tissues were removed from 6-week-old obese and lean mice after 2 h-restraint stress ($n = 8$), and then, analyzed by immunohistochemistry for fibrin as described in Materials and methods. Panels A and B: renal glomerulus of lean (A) and obese (B) mice after 2 h-restraint stress. An arrow denotes glomerular fibrin deposition in the stressed obese mouse (B). Magnification, ×400. Quantitative data were obtained by counting the number of glomeruli positive for fibrin out of at least 100 glomeruli in each kidney section and the percentage of the glomeruli positive for fibrin in each mouse was shown in (C).

mechanisms. We have previously studied the expression of PAI-1 in a mouse restraint-stress model, and revealed that stress-induced PAI-1 contributes to tissue thrombosis *in vivo* [21]. In this study, we investigated the effect of obesity on stress-induced PAI-1 expression and observed that PAI-1 expression was significantly increased by restraint stress in obese mice (Fig. 1–4; Table 1). Even restraint stress of short duration caused a dramatic induction of PAI-1 in the obese mice, which stood in marked contrast to the state of the lean mice (Fig. 1). Importantly, the adipose tissue of obese mice remarkably responded to stress in the synthesis of PAI-1 (Fig. 2; Table 1), resulting in a systemic prothrombotic state in the obese mice, as shown by the high levels of plasma PAI-1 [8]. Adipocytes, and the adipose tissue in general, are the principal site of PAI-1 production in obesity [7,10,26], and thus, obese animals may possess a large potential to synthesize PAI-1 in response to stress because of their abundant adipose mass, leading to a marked increase in systemic and regional anti-fibrinolytic activity.

More interestingly, the synthesis of PAI-1 in cardiac tissues was significantly increased by stress only in the obese mice (Fig. 3). This implies that PAI-1 response to stress in cardiac tissues may be modulated by obesity-linked hormonal abnormalities. *In situ* hybridization analysis showed that the increased signals for PAI-1 mRNA were localized in cardiovascular endothelial cells in the stressed obese mice (Fig. 3), i.e. in those cells in which inflammatory mediators could induce PAI-1 gene expression [12,16]. Cardiomyocytes are another source of heart PAI-1 *in vivo*, as shown in our previous study [27,28]. Taken together, these results suggest that the induction of cardiac PAI-1 may result in a decreased fibrinolytic potential in the heart of obese mice.

We have previously shown that acute inflammatory stress immediately caused PAI-1 mRNA induction in the kidney, resulting in the development of glomerular fibrin deposition [16]. We have demonstrated here the marked induction of PAI-1 mRNA in the kidneys of obese mice after short-duration restraint stress (Fig. 1). *In situ* hybridization analysis revealed that renal glomerular cells in obese mice specifically produced PAI-1 mRNA in response to stress (Fig. 4). Renal glomerular fibrin deposition was markedly induced by stress in obese mice (Fig. 5), suggesting that stress-mediated PAI-1 induction contributes to the suppression of systemic or regional fibrinolytic activity and to the development of tissue thrombosis. Increased dehydration by restraint stress did not seem to enhance fibrin deposition in obese mice because the elevation of hematocrit was < 5% after 2 h-restraint and not different between the obese and lean mice (data not shown).

Indeed, renal thrombosis was detected in morbid obesity in humans [29], and pathological changes such as glomerular capillary occlusion and fibrin cap are observed in diabetic nephropathy, which is often accompanied by obesity. However, our observations do not necessarily match the clinical situation in obese patients because stress-induced (arterial) thrombosis is frequently encountered in lung, heart, and brain. This discrepancy may be because of differences between species because murine models of hypercoagulability developed thrombi at unexpected sites where thrombosis rarely occurs in humans [30,31]. The development of thrombosis would be dependent upon the vascular-bed specific hemostatic balance

[32], which may explain why some organs do not develop thrombosis in this model. In any case, several reports describing a pathological role of PAI-1 for cardiovascular diseases in obese subjects [33] may support our finding that the systemic PAI-1 induction by stress can lead to tissue thrombosis in obese animals.

In conclusion, we have demonstrated here that obesity enhances the stress-mediated induction of the PAI-1 gene, which may contribute to renal fibrin deposition in stressed obese mice. The induction of cardiac PAI-1 expression in the stressed obese mice may be extrapolated to the high incidence of stress-associated cardiovascular disease in obese subjects. This study presents a possible molecular mechanism of stress-induced fibrin deposition in the tissue in obese conditions.

Acknowledgements

The authors thank T. Thinnes, T. Yamada, K. Kaneko, T. Nezu, and T. Nashida for their expert technical assistance. This work was supported by grants-in-aid from the Ministry of Education, Science, Sports and Culture, from the Ministry of Health and Welfare, Japan.

References

1 Larsson B. Obesity, fat distribution and cardiovascular disease. *Int J Obes* 1991; **15**: 53–7.
2 Bjontorp P. Abdominal fat distribution and disease: an overview of epidemiological data. *Ann Med* 1992; **24**: 15–8.
3 McGill JB, Schneider DJ, Arfken CL, Lucore CL, Sobel BE. Factors responsible for impaired fibrinolysis in obese subjects and NIDDM patients. *Diabetes* 1994; **43**: 104–9.
4 Potter van Loon BJ, Kluft C, Radder JK, Blankenstein MA, Meinders AE. The cardiovascular risk factor plasminogen activator inhibitor type 1 is related to insulin resistance. *Metab Clin Exp* 1993; **42**: 945–9.
5 Yamamoto K, Saito H. A pathological role of increased expression of plasminogen activator inhibitor-1 in human or animal disorders. *Int J Hematol* 1998; **68**: 371–85.
6 Kohler HP, Grant PJ. Plasminogen-activator inhibitor type 1 and coronary artery disease. *N Engl J Med* 2000; **342**: 1792–801.
7 Shimomura I, Funahashi T, Takahashi M, Maeda K, Kotani K, Nakamura T, Yamashita S, Miura M, Fukuda Y, Takemura K, Tokunaga K, Matsuzawa Y. Enhanced expression of PAI-1 in visceral fat: possible contributor to vascular disease in obesity. *Nat Med* 1996; **2**: 800–3.
8 Morange PE, Alessi MC, Verdier M, Casanova D, Magalon G, Juhan-Vague I. PAI-1 produced ex vivo by human adipose tissue is relevant to PAI-1 blood level. *Arterioscler Thromb Vasc Biol* 1999; **19**: 1361–5.
9 Samad F, Yamamoto K, Loskutoff DJ. Distribution and regulation of plasminogen activator inhibitor-1 in murine adipose tissue in vivo: induction by tumor necrosis factor-α and lipopolysaccharide. *J Clin Invest* 1996; **97**: 37–46.
10 Samad F, Loskutoff DJ. Tissue distribution and regulation of plasminogen activator inhibitor-1 in obese mice. *Mol Med* 1996; **2**: 568–82.
11 Konkle BA, Schuster SJ, Kelly MD, Harjes K, Hassett DE, Bohrer M, Tavassoli M. Plasminogen activator inhibitor-1 messenger RNA expression is induced in rat hepatocytes in vivo by dexamethasone. *Blood* 1992; **79**: 2636–42.
12 Samad F, Yamamoto K, Pandey M, Loskutoff DJ. Elevated expression of transforming growth factor-β in adipose tissue from obese mice. *Mol Med* 1997; **3**: 36–47.
13 Hotamisligil GS, Arner P, Caro JF, Atkinson RL, Spiegelman BM. Increased adipose tissue expression of tumor necrosis factor-α in human obesity and insulin resistance. *J Clin Invest* 1995; **95**: 2409–15.
14 Jern C, Eriksson E, Tengborn L, Risberg B, Wadenvik H, Jern S. Changes of plasma coagulation and fibrinolysis in response to mental stress. *Thromb Haemost* 1989; **62**: 767–71.
15 Takada Y, Urano T, Takahashi H, Nagai N, Takada A. Effects of electric footshock and water immersion restraint stresses on fibrinolytic parameters in the plasma of rats. *Thromb Res* 1998; **89**: 107–14.
16 Yamamoto K, Loskutoff DJ. Fibrin deposition in tissues from endotoxin-treated mice correlates with decreases in the expression of urokinase-type but not tissue-type plasminogen activator. *J Clin Invest* 1996; **97**: 2440–51.
17 Pinsky DJ, Liao H, Lawson CA, Yan S-H, Chen J, Carmeliet P, Loskutoff DJ, Stern DM. Coordinated induction of plasminogen activator inhibitor-1 (PAI-1) and inhibition of plasminogen activator gene expression by hypoxia promotes pulmonary vascular fibrin deposition. *J Clin Invest* 1998; **102**: 919–28.
18 Raikkonen K, Lassila R, Keltikangas-Jarvinen L, Hautanen A. Association of chronic stress with plasminogen activator inhibitor-1 in healthy middle-aged men. *Arterioscler Thromb Vasc Biol* 1996; **16**: 363–7.
19 Rosengren A, Hawken S, Ôunpuu S, Sliwa K, Zubaid M, Almahmeed WA, Blackett KN, Sitthi-amorn C, Sato H, Yusuf S. Association of psychosocial risk factors with risk of acute myocardial infarction in 11119 cases and 13648 controls from 52 countries (the INTERHEART study): case-control study. *Lancet* 2004; **364**: 953–62.
20 Glavin GB, Pare WP, Sandbak T, Bakke HK, Murison R. Restraint stress in biomedical research: an update. *Neurosci Biobehav Rev* 1994; **18**: 223–49.
21 Yamamoto K, Takeshita K, Shimokawa T, Yi H, Isobe K, Loskutoff DJ, Saito H. Plasminogen activator inhibitor-1 is a major stress-regulated gene: Implications for stress-induced thrombosis in aged individuals. *Proc Natl Acad Sci U S A* 2002; **99**: 890–5.
22 Lecomte D, Fornes P, Nicolas G. Stressful events as a trigger of sudden death: a study of 43 medico-legal autopsy cases. *Forensic Sci Int* 1996; **79**: 1–10.
23 Greenberg D, Ackerman SH. Genetically obese (ob/ob) mice are predisposed to gastric stress ulcers. *Behav Neurosci* 1984; **98**: 435–40.
24 Yamamoto K, Shimokawa T, Yi H, Isobe K, Kojima T, Loskutoff DJ, Saito H. Aging accelerates endotoxin-induced thrombosis: increased responses of plasminogen activator inhibitor-1 and LPS signaling with aging. *Am J Pathol* 2002; **161**: 1805–14.
25 Yamada T, Takagi A, Takeshita K, Yamamoto K, Ito M, Matsushita T, Murate T, Saito H, Kojima T. Enzyme immunoassay for measurement of murine plasminogen activator inhibitor-1, employing a specific antibody produced by DNA vaccines method. *Thromb Res* 2003; **111**: 285–91.
26 Lijnen HR, Maquoi E, Morange P, Voros G, Van Hoef B, Kopp F, Collen D, Juhan-Vague I, Alessi MC. Nutritionally induced obesity is attenuated in transgenic mice overexpressing plasminogen activator inhibitor-1. *Arterioscler Thromb Vasc Biol* 2003; **23**: 78–84.
27 Takeshita K, Yamamoto K, Ito M, Kondo T, Matsushita T, Hirai M, Kojima T, Nabeshima Y, Loskutoff DJ, Saito H, Murohara T. Increased expression of plasminogen activator inhibitor-1 with fibrin deposition in a murine model of aging, "*klotho*" mouse. *Semin Thromb Hemost* 2002; **28**: 545–53.
28 Takeshita K, Hayashi M, Iino S, Kondo T, Inden Y, Iwase M, Kojima T, Ito M, Loskutoff DJ, Saito H, Murohara T, Yamamoto K. Increased expression of plasminogen activator inhibitor-1 in cardiomyocytes contributes to cardiac fibrosis after myocardial infarction. *Am J Pathol* 2004; **164**: 449–56.
29 Luft FC, Walker PD, Hamburger RJ, Kleit SA. Thrombosis of the renal veins and vena cava. Occurrence in morbid obesity. *JAMA* 1975; **234**: 1158–60.

30 Erickson LA, Fici GJ, Lund JE, Boyle TP, Polites HG, Marotti KR. Development of venous occlusions in mice transgenic for the plasminogen activator inhibitor-1 gene. *Nature* 1990; **346**: 74–6.
31 Cui J, Eitzman DT, Westrick RJ, Christie PD, Xu ZJ, Yang AY, Purkayastha AA, Yang TL, Metz AL, Gallagher KP, Tyson JA, Rosenberg RD, Ginsburg D. Spontaneous thrombosis in mice carrying the factor V Leiden mutation. *Blood* 2000; **96**: 4222–6.
32 Rosenberg RD, Aird WC. Vascular-bed specific hemostasis and hypercoagulable states. *N Engl J Med* 1999; **340**: 1555–64.
33 Juhan-Vague I, Alessi MC, Mavri A, Morange PE. Plasminogen activator inhibitor-1, inflammation, obesity, insulin resistance and vascular risk. *J Thromb Haemost* 2003; **1**: 1575–9.

Journal of Thrombosis and Haemostasis, 4: 177–185

ORIGINAL ARTICLE

Fatal thrombosis of antithrombin-deficient mice is rescued differently in the heart and liver by intercrossing with low tissue factor mice

M. HAYASHI,* T. MATSUSHITA,† N. MACKMAN,‡ M. ITO,§ T. ADACHI,† A. KATSUMI,† K. YAMAMOTO,¶ K. TAKESHITA,* T. KOJIMA,** H. SAITO,†† T. MUROHARA* and T. NAOE†

**Department of Cardiology, Nagoya University Graduate School of Medicine; †Department of Hematology, Nagoya University Graduate School of Medicine; ‡Department of Immunology and Cell Biology, The Scripps Research Institute; §Department of Pathology, Nagoya University Hospital; ¶Department of Blood Transfusion Service, Nagoya University Hospital; **Department of Medical Technology, Nagoya University School of Health Sciences; and ††Nagoya Medical Center, Honshu, Japan*

To cite this article: Hayashi M, Matsushita T, Mackman N, Ito M, Adachi T, Katsumi A, Yamamoto K, Takeshita K, Kojima T, Saito H, Murohara T, Naoe T. Fatal thrombosis of antithrombin-deficient mice is rescued differently in the heart and liver by intercrossing with low tissue factor mice. *J Thromb Haemost* 2006; 4: 177–85.

Summary. *Background:* We previously reported that the targeted disruption of murine antithrombin (AT) gene resulted in embryonic lethality before 16.5 gestational days (gd) because of severe cardiac and hepatic thrombosis. *Objective and Methods:* To investigate the influences of lowered tissue factor (TF) activity upon hypercoagulation of $AT^{-/-}$ embryos, we crossed $AT^{+/-}$ with low TF ($mTF^{-/-}hTF^{+}$) mice to yield homozygous AT-deficient mice with the extremely low TF activity, that is expressed from the inserted human TF mini gene. *Results:* $AT^{-/-}$ embryos either with 50% TF ($AT^{-/-}mTF^{+/-}hTF^{+}$) or with low (~1% TF, $AT^{-/-}mTF^{-/-}hTF^{+}$) were not born, although the survival was prolonged until 18.5 gd. In both genotypes, histological examination showed disseminated thrombosis in hepatic sinusoidal space or in the portal veins, suggesting that the thrombogenesis caused loss of hepatic blood flow. As in original $AT^{-/-}$, $AT^{-/-}mTF^{+/-}hTF^{+}$ showed subcutaneous (s.c.) bleeding and also suffered from the myocardial degeneration apparently because of coronary thrombus formation. However, $AT^{-/-}mTF^{-/-}hTF^{+}$ had no skin hemorrhage and the thrombosis and degeneration were completely abolished in the heart. Myocardium of adult low TF mice had exhibited fibrosis secondary to hemorrhage; however, it was significantly decreased in low TF mice with $AT^{+/-}$. *Conclusions:* Our current model suggests that, in the heart, TF plays an important role in the thrombogenesis and it counterbalances AT-dependent anticoagulation. AT may be a potent anticoagulant during mice development and the activation and subsequent regulation of TF-procoagulant activity take place differently between the liver and the heart. These differences appear to point to local regulatory mechanisms in murine hemostasis.

Keywords: antithrombin, genetically altered mice, tissue factor.

Correspondence: Tadashi Matsushita, Department of Hematology, Nagoya University Graduate School of Medicine, 65-Tsurumai-cho, Showa-ku, Nagoya 466-8560, Japan.
Tel.: + 81 52 744 2145; fax: + 81 52 744 2161; e-mail: tmatsu@med.nagoya-u.ac.jp

Received 28 June 2005, accepted 2 September 2005

Introduction

Antithrombin (AT) is a plasma glycoprotein with a molecular weight of 58 000, one of the most important serine protease inhibitors of blood coagulation. AT inactivates thrombin and several serine proteases, including blood coagulation factors IXa, Xa, XIa, XIIa by forming a 1:1 molar complex between the active site of the serine protease and its reactive site. In the presence of heparan sulfate, the active site of the protease is brought into the close contact with the reactive site of AT, and the rate of inhibition is enhanced up to several thousand times [1–3].

Individuals deficient for AT are susceptible to venous thromboembolic diseases [4,5], but AT deficiency does not confer a predisposition to arterial thrombosis [6–8]. Nonetheless, such congenital patients are all heterozygous for its defect and individuals with an undetectable AT activity may not survive. We have generated AT-null mice through gene targeting and reported that homozygous null mice could not survive the prenatal period [9]. Extensive thrombosis occurred predominantly in the myocardium and liver sinusoids, and the embryos died before 16.5 gestational days (gd) along with massive s.c. bleeding. The skin bleeding was interpreted as arising from the consumption of coagulation factors. These results indicated the importance of AT in the anticoagulation in mouse embryo, but its organ-specific role was still unclear.

Tissue factor (TF) is a primary cellular initiator of blood coagulation. It is a transmembrane glycoprotein that binds

plasma FVII/FVIIa, that prototypically cleaves the substrates FIX and FX and initiates the coagulation protease cascade resulting in thrombin generation, fibrin deposition, and platelet activation [10,11]. TF is constitutively expressed at extravascular sites and plays an essential role in hemostasis by limiting the hemorrhage in the event of vascular injury [12].

Tissue factor is expressed during the early stages of both human and murine embryogenesis and targeted disruption of the murine TF (mTF) gene results in embryonic lethality between 9.5 and 10.5 gd [13–16]. The possible requirement of TF for embryogenesis, however, may be independent on signal transduction via TF cytoplasmic domain, as mice deficient for cytoplasmic domain are born and survive normally without any abnormalities in blood coagulation [17]. Nevertheless, prenatal lethality of complete TF deficiency in the early developmental stage appeared to limit the interpretation of TF importance in mammalian hemostasis and thrombogenesis. Previously, Parry *et al.* [18] developed transgenic mice named low TF mice ($mTF^{-/-}hTF^{+}$) and showed that fetal death could be rescued by expression of a human TF (hTF) cDNA at low levels (~1%: <0.1–1.0% of wild-type levels). The same rescuing effect was also accomplished by introducing minigenes without cytoplasmic domains. However, low TF mice had shorter life span and hemosiderin deposition and fibrosis secondary to hemorrhage of myocardium had been observed [18]. Hemodynamic studies had revealed that low TF mice had marked impairment of heart contractility [19]. These facts also suggested that TF has an pivotal role in the hemostasis of murine myocardial tissue.

The lethality of $AT^{-/-}$ embryos was because of unregulated coagulation activity and it is hypothesized that artificially reduced procoagulant activity may compensate such hemostatic unbalance. Low TF mice were crossed with $AT^{+/-}$ mice and studied whether lowering TF activity could affect the survival, and the degree of thrombosis of $AT^{-/-}$ mice. Additionally, we analyze whether bleeding in the heart of low TF mice is affected in the presence of 50% plasma AT levels that may attenuate the TF-dependent hemostasis in the heart.

Materials and methods

PCR

Each genotype was determined by PCR analyses of DNA eluted from the mouse tail. In mouse embryos, the lower limbs and tail were used. PCR for murine AT gene was performed with a forward primer (5′-CCTTCCAGACCGAACTGTCC) and a reverse primer (5′-GTAATCCCAGCCTTCTCCTG) to detect the expected deletion as previously described in Ref. [9]. For mTF gene, the PCR conditions were 33 cycles of denaturation for 1 min at 95 °C, annealing for 1 min at 65 °C, and extension for 1 min at 72 °C with a forward primer (5′-TTATAACGCACCCCGCGCCGACCCCGGC) and a reverse primer (5′-ACCGTGGGCGCGAGAGCCGCTAGGAGG). A forward primer (5′-CAAGATGGATTGCACGCAGGTTCTCC) and a reverse primer (5′-CACGAGGAAGCGGTCAGCCCATTGG) were used to detect *Neo* cassette, and a forward primer (5′-ATACATTCGAGTGCTCTGAAGTGCAT) and a reverse primer (5′-TGTTCGGGAGGGAATCACTGCTTGTTGAACA) were used for detection of hTF minigene.

Generation of AT-deficient mice with low TF activity

The generation of AT-deficient mice was described previously in Ref. [9]. Heterozygous AT-deficient mice were backcrossed to C57BL/6J congenic background for at least 10 generations. Low TF mice were generated as described earlier in Ref. [18] and transferred to Division of Experimental Animals, Center for Promotion of Medical Research and Education, Nagoya University. They have also been backcrossed to C57BL/6J. Experimental designs and protocols, including plasmid construction, generation of gene-targeting mice, were reviewed by the Nagoya University Animal Research Committee.

Strategy for breeding was summarized in Fig. 1 to generate AT-deficient mice with low TF activity. Females of low TF mice tend to suffer from the fatal bleeding complication during the gestational period. To avoid this, the female partner was set to having either $mTF^{+/+}$ or $mTF^{+/-}$ throughout the intercrossing. Here we used the notation $hTF^{+/-}$ for mice defined by breeding to contain a single copy of the human minigene and $hTF^{+/o}$ for mice that contain either one or two copies of the human minigene [20]. The first crossing was carried out between male $AT^{+/+}mTF^{-/-}hTF^{+/-}$ and female $AT^{+/-}mTF^{+/+}$ mice. Thereafter, mice heterozygous for AT and TF deficiency bearing hTF minigene, $AT^{+/-}mTF^{+/-}hTF^{+/-}$, were selected by PCR. Male or female $AT^{+/-}mTF^{+/-}hTF^{+/-}$ mice were then intercrossed and both $AT^{+/-}mTF^{-/-}hTF^{+/o}$ and $AT^{+/-}mTF^{+/-}hTF^{+/o}$ were further selected from the offsprings. Finally, pups between male $AT^{+/-}mTF^{-/-}hTF^{+/o}$ and female $AT^{+/-}mTF^{+/-}hTF^{+/o}$ mice were analyzed for the birth of pups with the expected genotypes. Thereafter, embryos of this intercrossing were collected at various times of gestation and subjected to the histological analysis (Table 1).

Two steps of intercrossing between mice bearing $hTF^{+/o}$ should result in the majority having two copies of hTF minigene both in $AT^{-/-}mTF^{+/-}hTF^{+/o}$ and $AT^{-/-}mTF^{-/-}hTF^{+/o}$. Indeed, mice were shown to have non-heterologous phenotype in terms of prenatal survival among the two genotype groups (see Results). *In vitro* studies had shown that TF activity was incomparable from the mice containing one or two copies of the minigene [20].

Histological analysis of embryos

At various times of gestation, females were sacrificed and the embryos were harvested and subjected to the histological analysis as described earlier in Refs. [9,21]. In brief, embryos were carefully dissected free of maternal tissue and a tail and a lower limb was used for genotyping by PCR analysis. Remaining tissues were washed three times in saline and fixed

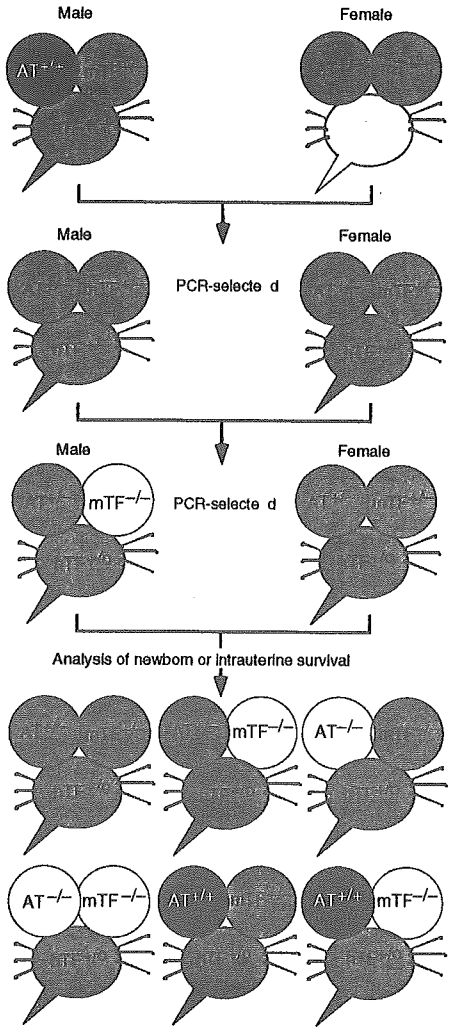

Fig. 1. Breeding strategy to generate AT-deficient mice with low TF activity. We used the notation $hTF^{+/-}$ for mice to contain a single copy of the human minigene and $hTF^{+/o}$ to contain either one or two copies of the human minigene [20] (see Materials and methods for details). Genetic status of AT, mTF, and hTF minigene was depicted in the right ear, left ear, and the face of mouse cartoon, respectively. Black-filled area denotes that both allele are present, whereas gray-shaded area denotes heterozygous status. Homozygous deficiency is represented by open white area. For status for hTF minigene, both $hTF^{+/-}$ and $hTF^{+/o}$ were denoted by gray-shaded face. To avoid bleeding complication of females with low TF, the female partner was usually set to having either $mTF^{+/+}$ or $mTF^{+/-}$. After the first crossing between male $AT^{+/+}mTF^{-/-}hTF^{+/-}$ and female $AT^{+/-}mTF^{+/+}$ mice, $AT^{+/-}mTF^{+/-}hTF^{+/-}$ was selected by the PCR and subsequently intercrossed. Finally, male $AT^{+/-}mTF^{-/-}hTF^{+/o}$ and female $AT^{+/-}mTF^{+/-}hTF^{+/o}$ mice were crossed and the birth of pups was analyzed for the six expected genotypes. Thereafter, embryos of this intercrossing were also collected and analyzed for intrauterine survival at various times of gestation (Table 1).

overnight in Carnoy's solution (methanol/chloroform/acetic acid = 6:3:1) and then dehydrated, embedded in paraffin, and sectioned (5-μm thick). Sections were stained with hematoxylin and eosin (H&E). For fibrin(ogen) immunohistochemical staining [22–24], slides were deparaffinized in xylene, transferred to 100% ethanol, and then incubated for 30 min in 0.3% H_2O_2/methanol. After rinsing with PBS, the slides were incubated successively with 5% normal goat serum/PBS (20 min, room temperature), rabbit antimouse fibrin(ogen) antibody DAKO 008 (Glostrup, Denmark; 1:200 dilution, overnight, 4 °C), antirabbit IgG Ab conjugated with biotin (1:500 dilution, 1 h, room temperature), and avidin–biotin complex conjugated with horseradish peroxidase (Vector Laboratories, Burlingame, CA, USA; 30 min, room temperature). Stained slides were visualized with diaminobenzidine tetrahydrochloride – Ni_3^+, CO_2^+ (Amersham Biosciences, Piscataway, NJ, USA).

The percent lesion of fibrin deposition was quantitated for the immunostained slides. Each pathomicrograph was scanned into a computer, and areas positive for fibrin(ogen) staining were calculated by using WinRoof, an image analysis software (Mitani Shoji, Tokyo, Japan). After establishing a color threshold, the lesion was extracted, then the percentage was calculated by dividing by the total heart or liver area. Margins or ventricular lumens of the heart were excluded from all the visual fields.

Evaluation of cardiac fibrosis

The quantitative measurement of cardiac fibrosis was according to the methods by Yoshiji, *et al.* [25]. $AT^{+/-}mTF^{-/-}hTF^{+}$ mice were analyzed according with low TF mice. Two groups were age-matched, and both were between 12 and 18 months old. The heart of sacrificed animals was quickly removed, then tissues were embedded in paraffin and stained with Azan–Mallory staining according with the control hematoxylin–eosin staining. Each pathomicrograph was scanned into a computer, and fibrotic areas positive for Azan–Mallory staining were calculated as described above. After establishing a color threshold, the blue color of the stained collagen fibers was extracted, the percentage of stained-fibers was calculated as described above.

Statistical analysis

Stat View 4.5 (SAS Institute Inc., Cary, NC, USA) was used for statistical analyses. The chi-squared tests were used to compare the distribution in each gestational age group. Student's *t*-test was used to compare the rates of myocardial fibrosis.

Results

Characterization of AT-null mice with lowered TF activity

Using targeted gene disruption, we previously generated AT-null mice and reported that 70% of $AT^{-/-}$ embryos died at 15.5 gd, while the remaining died at 16.5 gd, mainly because of hepatic and cardiac thrombosis [9]. Here we crossed $AT^{+/-}$ with low TF mice, which lack the mTF gene but contain the hTF minigene (Fig. 1), expressing ~1% TF activity [18].

Table 1 Genotypes of living embryos derived through mating between $AT^{+/-}$ $mTF^{-/-}$ $hTF^{+/o}$ and $AT^{+/-}$ $mTF^{+/-}$ $hTF^{+/o}$

Gestational day	Genotype*						*n*
	$AT^{+/-}mTF^{+/-}$	$AT^{+/-}mTF^{-/-}$	$AT^{-/-}mTF^{+/-}$	$AT^{-/-}mTF^{-/-}$	$AT^{+/+}mTF^{+/-}$	$AT^{+/+}mTF^{-/-}$	
19.5†	28 (37.3%)	13 (17.3%)	0 (0%)	4 (5.3%)	15 (20%)	15 (20%)	75
18.5	12 (27.3%)	10 (22.7%)	4 (9.1%)	7 (15.9%)	7 (15.9%)	4 (9.1%)	44
17.5	20 (33.8%)	17 (28.8%)	7 (11.9%)	3 (5.1%)	5 (8.5%)	7 (11.9%)	59
16.5	14 (38.9%)	7 (19.4%)	4 (11.1%)	3 (8.3%)	6 (16.7%)	2 (5.6%)	36
15.5	7 (21.9%)	6 (18.8%)	4 (12.5%)	4 (12.5%)	8 (25%)	3 (9.4%)	32
Expected	25%	25%	12.50%	12.50%	12.50%	12.50%	

*Genotype of each offspring is depicted without showing '$hTF^{+/o}$.' Values in parenthesis are the percentage of each birth. †The frequency of live embryos with either $AT^{-/-}mTF^{+/-}$ or $AT^{-/-}mTF^{-/-}$ was significantly smaller than the expected one in four (chi-squared $P = .0007$ for $mTF^{+/-}$ status and $P = 0.013$ for $mTF^{-/-}$ status, respectively). At other gestational days except for 19.5 gd, the observed frequencies were not different from the expected frequencies by chi-squared test.

We analyzed over three-hundred offsprings between $AT^{+/-}$ $mTF^{-/-}hTF^{+/o}$ and $AT^{+/-}mTF^{+/-}hTF^{+/o}$ mice and found that there were no living pups carrying the expected $AT^{-/-}$ genotypes; i.e. $AT^{-/-}mTF^{+/-}hTF^{+/o}$ (about 50% TF activity) or $AT^{-/-}mTF^{-/-}hTF^{+/o}$ (a trace amount of TF activity) (not shown). Therefore, even if TF activity was reduced to extremely low levels, the prenatal lethality of $AT^{-/-}$ mice could not be rescued.

To elucidate the cause of embryonic lethality, total of 246 living embryos between $AT^{+/-}mTF^{-/-}hTF^{+/o}$ and $AT^{+/-}mTF^{+/-}hTF^{+/o}$ mice were collected at various times of gestation. Living embryos were determined by their heart beating and the genotype of each embryo was determined by PCR analysis. The observed frequencies of living embryos were compared with the expected Mendelian ratios (Table 1). The PCR analysis detected hTF minigene and there were no embryos with $mTF^{-/-}hTF^{-/-}$ genotypes. We could not find the living embryos with either $AT^{-/-}$ genotypes after 20.5 gd (not shown). However, at each gestational day before 19.5 gd, the observed frequencies of all the genotypes were not statistically different from the expected frequencies by chi-squared test. At 19.5 gd, there were no $AT^{-/-}mTF^{+/-}hTF^{+/o}$ embryos and the frequency of live embryos with either $AT^{-/-}$ genotype ($AT^{-/-}mTF^{+/-}hTF^{+/o}$ and $AT^{-/-}mTF^{-/-}hTF^{+/o}$) was smaller than the expected one in four (chi-squared $P = .0007$ for $mTF^{+/-}hTF^{+/o}$ status and $P = .013$ for $mTF^{-/-}hTF^{+/o}$ status, respectively). These facts suggest that $AT^{-/-}$ embryos with reduced TF levels had longer intrauterine survival.

Dead embryos with $AT^{-/-}mTF^{+/+}$ had shown hemorrhagic skin and it was extensive s.c. hemorrhage [9]. Before 17.5 gd, there were no embryos with hemorrhagic skin, but after 17.5 gd, we also found that eight $AT^{-/-}mTF^{+/-}hTF^{+/o}$ embryos displayed hemorrhagic skin and six of them had no heart beating. Figure 2A shows live $AT^{-/-}mTF^{+/-}hTF^{+/o}$ embryos at 18.5 gd with severe s.c. hemorrhage, but no fibrin deposition was apparent by immunohistochemical staining of the whole body (data not shown). In contrast, none of dead or live $AT^{-/-}mTF^{-/-}hTF^{+/o}$ embryos exhibited s.c. hemorrhage (Fig. 2B).

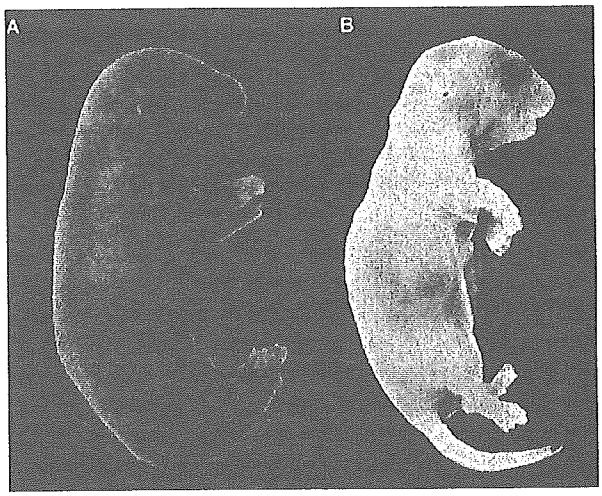

Fig. 2. Macroscopic observation of $AT^{-/-}mTF^{+/-}hTF^{+/o}$ (A) and $AT^{-/-}mTF^{-/-}hTF^{+/o}$ (B) embryos at 18.5 gd. Eight $AT^{-/-}mTF^{+/-}hTF^{+/o}$ embryos showed extensive hemorrhage between 17.5 and 19.5 gd as represented in (A) and only two were alive (see Results for detail). $AT^{-/-}mTF^{-/-}hTF^{+/o}$ embryos did not show s.c. hemorrhage (B).

Cardiac thrombosis of AT-null embryos with reduced TF activity

Mice embryos were examined histologically with H&E staining according with fibrin(ogen) immunostaining [22–24] that detects tissue fibrin deposition in various embryonal organs. Our previous findings had indicated that AT-null mice exhibited the fibrin deposition in the degenerated myocardium, beginning after 14.5 gd [9]. In $AT^{-/-}mTF^{+/-}hTF^{+/o}$, myocardial fibrin deposition was partially found from 16.5 gd (data not shown). After 16.5 gd, in all of this genotype, we found myocardial degeneration according with minor bleeding (Fig. 3A) and fibrin(ogen) immunostaining demonstrated that fibrin deposition was found in the degenerated lesion (Fig. 3B). In some embryos, large thrombi were found in the left heart auricle (Fig. 3C). The thrombi appeared to be easily formed in the left atria probably because blood flow is low in fetal

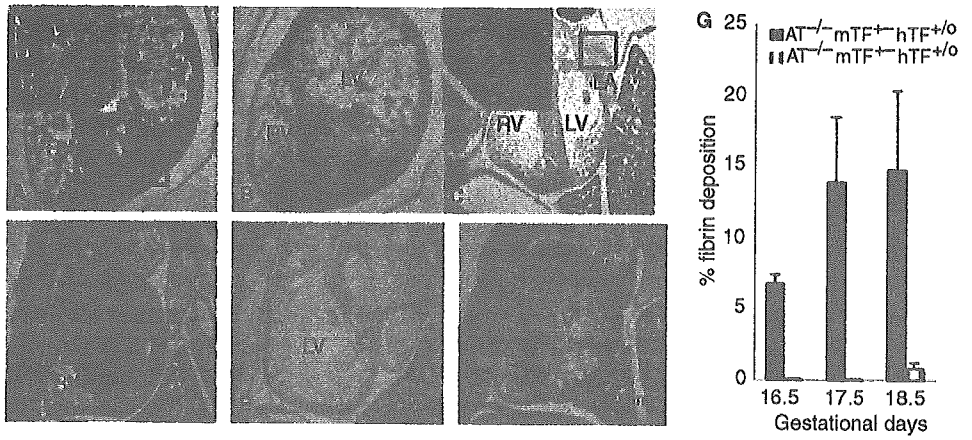

Fig. 3. Microscopic observations of embryonal myocardium. H&E staining (A, C, D, and F) or antifibrin(ogen) immunostaining (B and E) is shown for $AT^{-/-}mTF^{+/-}hTF^{+/o}$ at 17.5 gd (A–C) and $AT^{-/-}mTF^{-/-}hTF^{+/o}$ at 18.5 gd (D–F). Immunochemical staining was performed with antifibrin(ogen) antibody as described in Materials and methods. (A) Myocardial degeneration and partial necrosis were found in all of this genotype, according with the minor bleeding (◀). Inset shows high magnification of boxed area (×200). (B) Fibrin deposition, within degenerated areas, that occupies anterior, septal and partially posterior, but not lateral wall of the left ventricle. (C) A large thrombus in the left atrium (box) and is magnified in inset with ×200. (D–F) $AT^{-/-}mTF^{-/-}hTF^{+/o}$ embryos exhibit no thrombus formation in myocardium or left atrium either by H&E (D, F) or antifibrin(ogen) immunostaining (E). In panels E–F, erythrocyte pool remains in LV: left ventricle; LA: left atrium; and RV: right ventricle, while no thrombus or immunoreactive fibrin(ogen) is found. In (A)–(F), Magnification is ×40 except for inset. (G) Percent fibrin deposition was calculated as described in Materials and methods. Values are means and standard errors obtained from three living $AT^{-/-}mTF^{-/-}hTF^{+}$ or $AT^{-/-}mTF^{+/-}hTF^{+/o}$ mice at each indicated gestational day (16.5–18.5 gd). Few area of fibrin deposition were observed in $AT^{-/-}mTF^{-/-}hTF^{+/o}$ mice.

circulation. We also confirmed that atrial thrombi were found in $AT^{-/-}mTF^{+/+}$ embryos after 16.5 gd (data not shown).

Additionally, we found that the myocardial degeneration was segmental to coronary circulation. Figure 3B, for instance, indicated that fibrin deposition was formed in anterior, septal and partially posterior, but not in lateral wall of the left ventricle. Figure 4 indicated the thrombus in the small coronary vessel of living $AT^{-/-}mTF^{+/-}hTF^{+/o}$ embryo at 17.5 gd.

In contrast, the heart specimens from 21 living $AT^{-/-}mTF^{-/-}hTF^{+/o}$ embryos showed no obvious pathological abnormalities (Fig. 3D and F). Fibrin(ogen) immunostaining failed to detect the cardiac thrombosis from any specimens (Fig. 3E). We calculated the percent lesion of fibrin deposition detected by fibrin(ogen) immunostaining and found that the cardiac fibrin deposition was almost absent in $AT^{-/-}mTF^{-/-}hTF^{+/o}$ embryos (Fig. 3G). Therefore, when TF activity was abundantly lowered to ~1%, development of the cardiac thrombosis was abolished in AT-null embryos.

Liver thrombosis of AT-null embryos with reduced TF activity

$AT^{-/-}mTF^{+/+}$ also had thrombus in liver, and diffuse fibrin deposition was observed mainly in perisinusoidal space, starting from 15.5 gd [9]. There were no thrombotic changes in hepatic central veins. In the current study, both $AT^{-/-}mTF^{+/-}hTF^{+/o}$ and $AT^{-/-}mTF^{-/-}hTF^{+/o}$ embryos had similar hepatic changes and thrombi also were found in the portal veins but not in central veins (Fig. 5A–D). Figure 5E and F indicated that various extent of hepatic necrosis was observed after 15.5 gd. Figure 5G compared the degree of liver thrombosis between $AT^{-/-}mTF^{-/-}hTF^{+/o}$ and $AT^{-/-}mTF^{+/}$

Fig. 4. Coronary thrombosis of the $AT^{-/-}mTF^{+/-}hTF^{+/o}$ embryo. A representative image of H&E staining of myocardium from $AT^{-/-}mTF^{+/-}hTF^{+/o}$ at 17.5 gd shows a thrombus in a small coronary vessel (boxed area) located in subepicardium of the left ventricular lateral wall. Magnification is ×160 and inset magnifies the boxed area with ×640. *, degenerated cardiac tissue; **, necrotic cardiac tissue; #, normal cardiomyocyte.

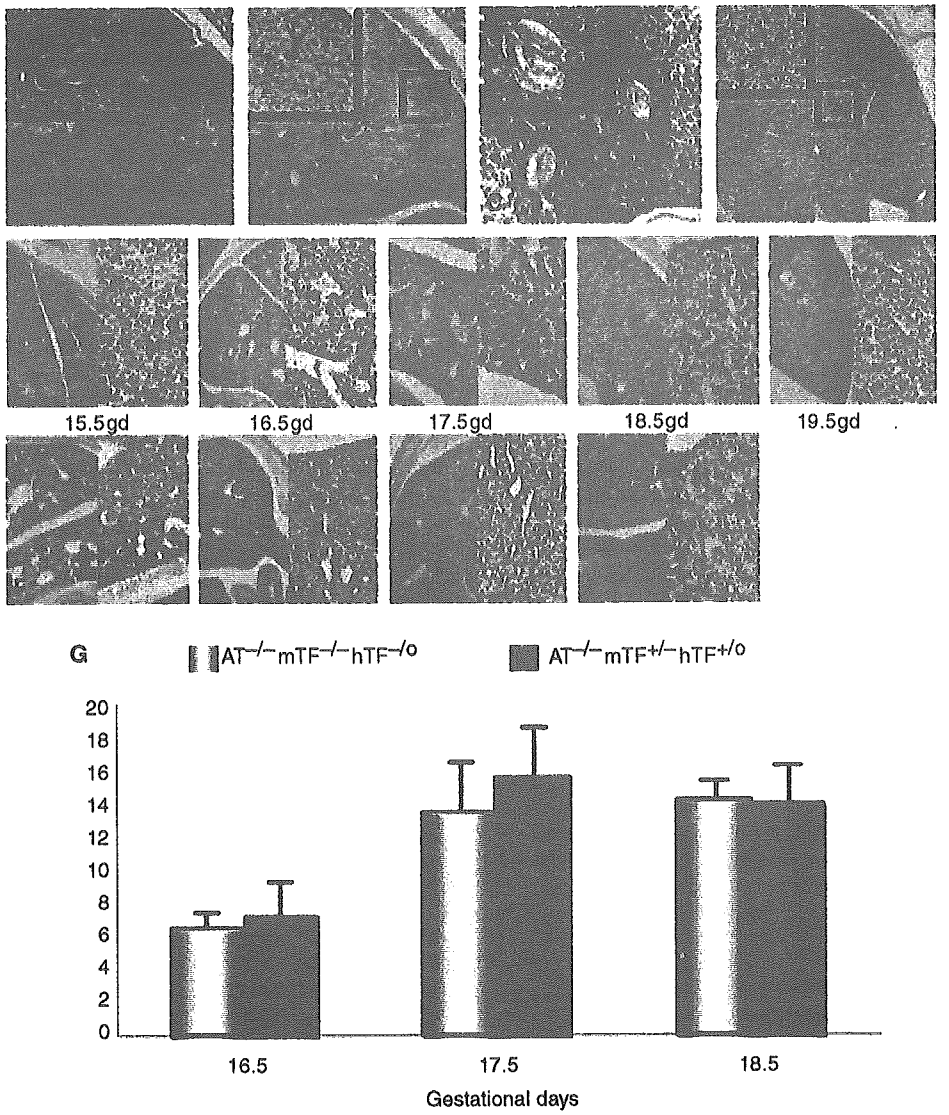

Fig. 5. Microscopic observations of the liver of $AT^{-/-}mTF^{+/-}hTF^{+/o}$ and $AT^{-/-}mTF^{-/-}hTF^{+/o}$ embryos. Panels A–D denote hepatic thrombosis in the embryo of $AT^{-/-}mTF^{-/-}hTF^{+/o}$ (A and B) or $AT^{-/-}mTF^{+/-}hTF^{+/o}$ (C and D) at 18.5 gd. H&E staining indicates large thrombus found in the intrahepatic portal vein from both genotypes (A and C). Diffuse fibrin deposition was detected in the sinusoidal space from both genotypes (B and D). Magnification: ×40. Inset magnifies boxed areas with ×200. (E and F) Time course of fibrin deposition in liver on the indicated gestational days by antifibrin(ogen) immunostaining. In E (living $AT^{-/-}mTF^{-/-}hTF^{+/o}$) and F ($AT^{-/-}mTF^{+/-}hTF^{+/o}$), each left sub-panel denotes diffuse hepatic fibrin deposition (×40 magnification) and the right sub-panel shows the close-up view of the thrombotic lesions by ×160 magnification. No embryos were living of $AT^{-/-}mTF^{+/-}hTF^{+/o}$ at 19.5 gd and were not available for the analysis. (G) The percent lesion with immunoreactive fibrin was calculated as described in the legend to Fig. 3 and compared between the liver specimen from $AT^{-/-}mTF^{-/-}hTF^{+/o}$ and $AT^{-/-}mTF^{+/-}hTF^{+/o}$. Values are means and standard errors obtained from three living $AT^{-/-}mTF^{-/-}hTF^{+}$ or $AT^{-/-}mTF^{+/-}hTF^{+/o}$ mice and no significant differences were observed at each indicated gestational day. Antifibrin(ogen) immunostaining (B, D, E, and F) was performed as described in the legend to Fig. 3.

$^{-}hTF^{+/o}$ by calculating the area positive for fibrin(ogen) immunostaining. The amount of sinusoidal fibrin deposition was the same in both genotypes and increased in intrauterine growth-dependent manner. Therefore, liver thrombosis appeared to have fatal effect both on $AT^{-/-}mTF^{+/-}hTF^{+/o}$ and $AT^{-/-}mTF^{-/-}hTF^{+/o}$. In other embryonal tissues, including brain, lung, and kidney, no fibrin deposition was detected by careful observation of immunohistochemical staining of whole body specimen (not shown).

Heterozygous AT deficiency improves cardiac fibrosis of low TF mice

Low TF mice had left ventricular dysfunction because of cardiac fibrosis that appears to be caused by minor hemorrhage, resulting in their shorter life span [19]. We also observed that cardiac fibrosis occurred in low TF mice ($AT^{+/+}mTF^{-/-}hTF^{+/o}$) and the fibrosis was extensive after 12 months old (Fig. 6A), while their littermate $AT^{+/-}mTF^{-/-}hTF^{+/o}$ showed

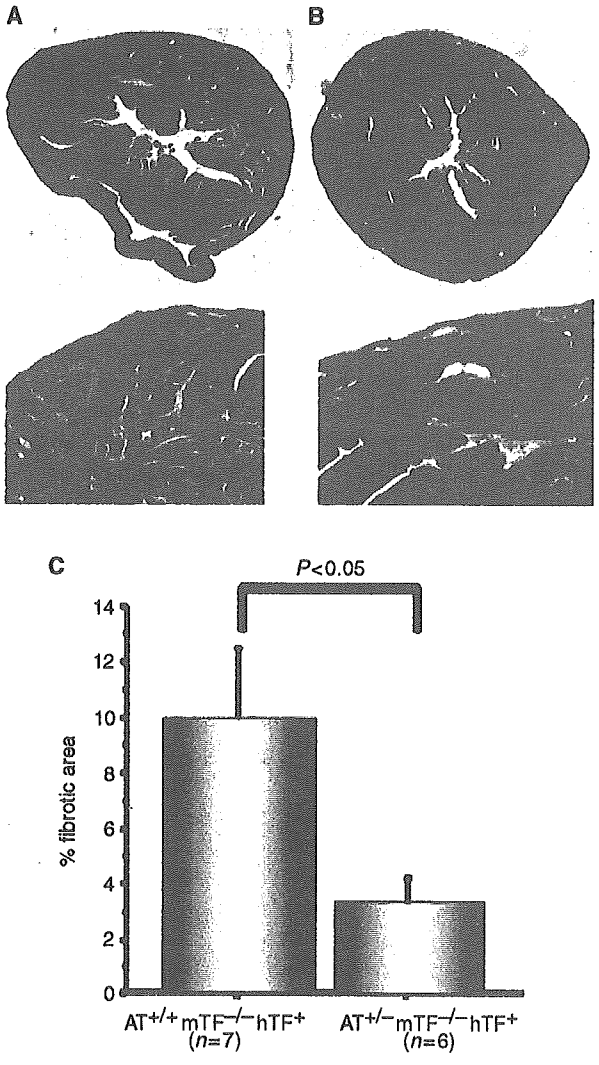

Fig. 6. Comparison of cardiac fibrosis between low TF mice and low TF mice with ~50% AT activity. Fibrotic areas were stained in blue with Azan–Mallory staining according with hematoxylin–eosin staining as described in Materials and methods. In an $AT^{+/+}mTF^{-/-}hTF^{+/o}$ mouse (low TF mice, panel A) and its littermate $AT^{+/-}mTF^{-/-}hTF^{+/o}$ (panel B) of 12 months old, horizontal section of the heart was shown by ×25 magnification (upper sub-panel) with a representative fibrotic area (lower sub-panel, ×100 magnification). (C) Percent fibrotic area was measured as described in Materials and methods, and the cardiac fibrosis is significantly decreased in $AT^{+/-}mTF^{-/-}hTF^{+/o}$ mice ($P < 0.05$). Values are means and SD obtained from 12–18-month-old $AT^{+/+}mTF^{-/-}hTF^{+/o}$ mice ($n = 7$) or their littermate $AT^{+/-}mTF^{-/-}hTF^{+}$ ($n = 6$).

decreased myocardial fibrosis (Fig. 6B). We quantitated the percent lesion of fibrosis in the assigned areas of myocardium both in 12–18-month-old $AT^{+/-}mTF^{-/-}hTF^{+/o}$ ($n = 6$) and their littermate $AT^{+/+}mTF^{-/-}hTF^{+/o}$ mice ($n = 7$). The degree of cardiac fibrosis was significantly reduced in $AT^{+/-}mTF^{-/-}hTF^{+/o}$ mice (Fig. 6C), suggesting that heterozygous for AT deficiency with ~50% AT levels protected the myocardium from fibrosis.

Discussion

Our mouse model suggest the requirement of the two procoagulant and anticoagulant proteins during the mouse development, although embryonal hemostasis may differ between various mammalian species. Previously, we observed that AT-null embryos exhibited fibrin deposition and degeneration in myocardium and liver [9]. The current study indicated that the site of thrombosis of AT-null embryos was also limited to the heart and liver. These facts suggested that AT has particular roles in the control of thrombogenesis of the two organs during mouse embryogenesis. Our analysis of over two-hundred embryos between male $AT^{+/-}mTF^{-/-}hTF^{+/o}$ and female $AT^{+/-}mTF^{+/-}hTF^{+/o}$ indicated that a reduction of TF activity failed to rescue the lethality, but prolonged the survival of AT-null embryos by several days (Table 1).

We examined the hearts from the total of 21 embryos of AT-null with low TF activity ($AT^{-/-}mTF^{-/-}hTF^{+/o}$) and no pathological abnormality was detected (Fig. 3), indicating that reduction of TF activity to extremely low levels could relieve from the cardiac thrombosis, whereas about 50% reduction could not (Fig. 3). Apparently, in the heart, hypercoagulable state of AT-null embryos appeared to be balanced by the absence of TF-initiated activation of coagulation proteases. In our timed mating, no embryos could be produced with $AT^{-/-}mTF^{+/+}$ but the comparison with our previous observation suggested that the occurrence of cardiac thrombosis appeared to delay in 1–2 days in $AT^{-/-}mTF^{+/-}hTF^{+/o}$ mice. We also found four living embryos with $AT^{-/-}mTF^{-/-}hTF^{+/o}$ at 19.5 gd. It is therefore possible that the delayed or absence of cardiac thrombosis and degeneration might benefit the slight life prolongation of AT-null embryos.

In $AT^{-/-}mTF^{+/-}hTF^{+/o}$ embryos, thrombi were found in small coronary arteries (Fig. 4) and the pattern of fibrin deposition was segmental to irrigation by the coronary artery flow (Fig. 3B), suggesting that the complete AT deficiency may lead to thrombus formation in cardiac vessels followed by ischemic myocardial damage. Previously, several studies of ischemia-reperfusion (I/R) injury models of adult animals had found the increased TF activity [26] or increased TF mRNA, antigen, and activity [27], suggesting that ischemic damage results in higher TF expression in cardiomyocytes. Also, damage to the endothelial barrier would permit the plasma clotting factors to gain access to TF expressed by the extravascular cardiomyocytes, probably leading to local thrombin generation and fibrin deposition. We also observed myocardial degeneration according to bleeding, and thus fibrin deposition might also have in part resulted from microvascular bleeding in degenerated myocardium. Therefore, AT would have been needed to protect from the unregulated thrombin generation, and probably from the fibrin deposition in the myocardium of AT-null mice. At present, however, thrombi were found only in middle-smaller-sized vessels and it is not determined whether larger coronary arteries were affected as in conventional myocardial infarction of human adults.

In turn, the principal role of TF in the hemostasis of the heart has been suggested by the fact that the heart from elderly low TF mice had shown extensive fibrosis secondary to the hemorrhage of myocardium [19]. Interestingly, our experiment indicated that the fibrosis of low TF mice was significantly decreased by heterozygous AT deficiency (Fig. 6). Thus, our current study suggest that AT anticoagulation system is fitted to hemostatic balance of the murine heart in terms of counterbalancing of the TF-initiated thrombin generation.

Unlike our intercrossing between AT-null and low TF mice, another intercrossing resulted in the successful rescue of lethality of mice deficient for a potent anticoagulant. Mice deficient for TFPI suffered from disseminated thrombosis and are embryonic lethal apparently because of the intracranial hemorrhage [28]. Crossbreeding with low TF mice completely rescued the lethal thrombogenesis of TFPI-null mice [20], demonstrating its role as a specific antagonist of TF-initiated coagulation. In turn, decreases in TFPI levels did not rescue the fibrotic myocardium followed by the repeated hemorrhagic events of low TF mice [20], presenting a good contrast with our finding. Such difference is in part dependent on possibly distinct magnitude of anticoagulant roles of the two proteins in the heart, nonetheless which is totally unknown. At least, unlike AT-null mice, cardiac thrombosis has not been described in TFPI-null mice [28] and TFPI may have less important roles in antithrombogenesis in the murine heart.

By contrast to the findings in the heart, hepatic thrombus formation and necrosis were observed by the gestational age-dependent manner from AT-null mice having either TF genotype (Fig. 5). In embryonal circulation, the portal system is connected to the umbilical artery and placenta. Fibrin deposition was detected in liver sinusoids, but not in the central veins (Fig. 5A–D), therefore, thrombosis in the portal system might cause severe hepatic dysfunction of the embryos. Thus, development of massive liver thrombosis may be critical for life of the embryos.

In $AT^{-/-}mTF^{-/-}hTF^{+/o}$ embryos, the marked difference of occurrence of thrombosis between the heart and liver remains unexplained. However, a study compared sodium dodecyl sulphate (SDS)-soluble extracts of various human organs and found that AT is predominated in liver compared with other organs [29]. AT acts more efficiently in the presence of heparan sulfate and thus AT deficiency might be profound in the organ that is rich in endothelium-based heparan sulfate proteoglycan. Indeed, heparan sulfate exhibits an unusually high degree of sulfation from the liver compared with other tissues, that is crucial for interaction with AT [30]. In this context, guard from thrombogenesis may be more dependent on AT that tightly associates with heparan sulfate of the hepatic vascular bed.

Liver is composed by various cell types including Kupfer cells that predominantly express TF on its cell surface. However, low TF mice did not have the bleeding in the liver and mTF mRNA expression was lower in the liver than in the heart [18], although it is not known whether liver is insignificant for TF-dependent activation of coagulation cascades. In this situation, differences in TF impact on liver thrombogenesis might result in different rescue of thrombosis in AT-null mice, although the entire reasons should need further studies including careful observation of spatial distribution of cellular TF.

We had observed that all the dead $AT^{-/-}mTF^{+/+}$ embryos had shown extensive s.c. hemorrhage [9], but we could find that only eight embryos (two living) showed skin hemorrhage with $AT^{-/-}mTF^{+/-}hTF^{+/o}$ genotype. Because we observed that most of the living embryos did not show skin hemorrhage, it might occur at the critical period of death and the hemorrhage is probably not necessarily related to the cause of death. Interestingly, skin hemorrhage was not found in $AT^{-/-}mTF^{-/-}hTF^{+/o}$ at any gestational ages (Fig. 2B), suggesting that the hemorrhage appeared to be attenuated by lowering the TF levels. Currently, we have found no fibrin deposition subcutaneously from any mouse genotypes (not shown), and the consumption of coagulation factors may underlie the s.c. hemorrhage because of massive thrombus formation. Absolutely, it could not be measured whether fibrinogen or other coagulation factors were decreased in the embryonal plasma and the cause of the s.c. hemorrhage is not entirely determined.

Authorship details

Mutsuharu Hayashi: tissue section preparation and HE staining, writing, data analysis and interpretation; Tadashi Matsushita: data interpretation and writing; Nigel Mackman: low TF mice provision and supervision of manuscript; Masafumi Ito: fibrinogen immunostaining and interpretation of organ pathology; Tatsuya Adachi: PCR analysis of mouse tail DNA and plaque check plus general mice maintenance; Kyosuke Takeshita: instruction of experimentation (MH) especially for general animal manipulation and PCR; Koji Yamamoto: PCR analysis of mouse tail DNA; Akira Katsumi: statistical analysis, supervision and manuscript revision; Tetsuhito Kojima: PCR Primer design and writing; Hidehiko Saito: conception of project and supervision; Toyoaki Murohara and Tomoki Naoe: coordination of project and manuscript writing.

Acknowledgements

This work was supported in part by grants-in-aid No. 16590933 from Japan Society for the Promotion of Science (TM), and also from the Japanese Ministry of Health, Labor and Welfare (TK). We especially give many thanks to Dr Masamitsu Yanada for his corporations and helpful advices. We thank Keiko Kinoshita, Tomoyo Nezu, Makoto Ikejiri, Takayuki Yamada, and Takashi Iwasaki for their excellent technical assistance.

References

1 Bauer KA, Rosenberg RD. Role of antithrombin III as a regulator of in vivo coagulation. *Semin Hematol* 1991; **28**: 10–8.
2 Blajchman MA, Austin RC, Fernandez-Rachubinski F, Sheffield WP. Molecular basis of inherited human antithrombin deficiency. *Blood* 1992; **80**: 2159–71.

3 Pratt CW, Church FC. Antithrombin: structure and function. *Semin Hematol* 1991; **28**: 3–9.

4 Lane DA, Kunz G, Olds RJ, Thein SL. Molecular genetics of antithrombin deficiency. *Blood Rev* 1996; **10**: 59–74.

5 Bayston TA, Lane DA. Antithrombin: molecular basis of deficiency. *Thromb Haemost* 1997; **78**: 339–43.

6 Greaves M, Preston FE. The hypercoagulable state in clinical practice. *Br J Haematol* 1991; **79**: 148–51.

7 Thomas DP, Roberts HR. Hypercoagulability in venous and arterial thrombosis. *Ann Intern Med* 1997; **126**: 638–44.

8 De Stefano V, Finazzi G, Mannucci PM. Inherited thrombophilia: pathogenesis, clinical syndromes, and management. *Blood* 1996; **87**: 3531–44.

9 Ishiguro K, Kojima T, Kadomatsu K, Nakayama Y, Takagi A, Suzuki M, Takeda N, Ito M, Yamamoto K, Matsushita T, Kusugami K, Muramatsu T, Saito H. Complete antithrombin deficiency in mice results in embryonic lethality. *J Clin Invest* 2000; **106**: 873–8.

10 Edgington TS, Mackman N, Brand K, Ruf W. The structural biology of expression and function of tissue factor. *Thromb Haemost* 1991; **66**: 67–79.

11 Nemerson Y. Tissue factor and hemostasis. *Blood* 1988; **71**: 1–8.

12 Drake TA, Morrissey JH, Edgington TS. Selective cellular expression of tissue factor in human tissues. Implications for disorders of hemostasis and thrombosis. *Am J Pathol* 1989; **134**: 1087–97.

13 Luther T, Flossel C, Mackman N, Bierhaus A, Kasper M, Albrecht S, Sage EH, Iruela-Arispe L, Grossmann H, Strohlein A, Zhang Y, Nawroth PP, Carmeliet P, Loskutoff DJ, Muller M. Tissue factor expression during human and mouse development. *Am J Pathol* 1996; **149**: 101–13.

14 Toomey JR, Kratzer KE, Lasky NM, Stanton JJ, Broze Jr GJ. Targeted disruption of the murine tissue factor gene results in embryonic lethality. *Blood* 1996; **88**: 1583–7.

15 Bugge TH, Xiao Q, Kombrinck KW, Flick MJ, Holmback K, Danton MJ, Colbert MC, Witte DP, Fujikawa K, Davie EW, Degen JL. Fatal embryonic bleeding events in mice lacking tissue factor, the cell-associated initiator of blood coagulation. *Proc Natl Acad Sci USA* 1996; **93**: 6258–63.

16 Carmeliet P, Mackman N, Moons L, Luther T, Gressens P, Van Vlaenderen I, Demunck H, Kasper M, Breier G, Evrard P, Muller M, Risau W, Edgington T, Collen D. Role of tissue factor in embryonic blood vessel development. *Nature* 1996; **383**: 73–5.

17 Melis E, Moons L, De Mol M, Herbert JM, Mackman N, Collen D, Carmeliet P, Dewerchin M. Targeted deletion of the cytosolic domain of tissue factor in mice does not affect development. *Biochem Biophys Res Commun* 2001; **286**: 580–6.

18 Parry GC, Erlich JH, Carmeliet P, Luther T, Mackman N. Low levels of tissue factor are compatible with development and hemostasis in mice. *J Clin Invest* 1998; **101**: 560–9.

19 Pawlinski R, Fernandes A, Kehrle B, Pedersen B, Parry G, Erlich J, Pyo R, Gutstein D, Zhang J, Castellino F, Melis E, Carmeliet P, Baretton G, Luther T, Taubman M, Rosen E, Mackman N. Tissue factor deficiency causes cardiac fibrosis and left ventricular dysfunction. *Proc Natl Acad Sci USA* 2002; **99**: 15333–8.

20 Pedersen B, Holscher T, Sato Y, Pawlinski R, Mackman N. A balance between tissue factor and tissue factor pathway inhibitor is required for embryonic development and hemostasis in adult mice. *Blood* 2005; **105**: 2777–82.

21 Yanada M, Kojima T, Ishiguro K, Nakayama Y, Yamamoto K, Matsushita T, Kadomatsu K, Nishimura M, Muramatsu T, Saito H. Impact of antithrombin deficiency in thrombogenesis: lipopolysaccharide and stress-induced thrombus formation in heterozygous antithrombin-deficient mice. *Blood* 2002; **99**: 2455–8.

22 Wilhelm O, Hafter R, Coppenrath E, Pflanz MA, Schmitt M, Babic R, Linke R, Gossner W, Graeff H. Fibrin-fibronectin compounds in human ovarian tumor ascites and their possible relation to the tumor stroma. *Cancer Res* 1988; **48**: 3507–14.

23 Moons L, Shi C, Ploplis V, Plow E, Haber E, Collen D, Carmeliet P. Reduced transplant arteriosclerosis in plasminogen-deficient mice. *J Clin Invest* 1998; **102**: 1788–97.

24 Wang J, Zheng H, Ou X, Albertson CM, Fink LM, Herbert JM, Hauer-Jensen M. Hirudin ameliorates intestinal radiation toxicity in the rat: support for thrombin inhibition as strategy to minimize side-effects after radiation therapy and as countermeasure against radiation exposure. *J Thromb Haemost* 2004; **2**: 2027–35.

25 Yoshiji H, Buck TB, Harris SR, Ritter LM, Lindsay CK, Thorgeirsson UP. Stimulatory effect of endogenous tissue inhibitor of metalloproteinases-1 (TIMP-1) overexpression on type IV collagen and laminin gene expression in rat mammary carcinoma cells. *Biochem Biophys Res Commun* 1998; **247**: 605–9.

26 Golino P, Ragni M, Cirillo P, Avvedimento VE, Feliciello A, Esposito N, Scognamiglio A, Trimarco B, Iaccarino G, Condorelli M, Chiariello M, Ambrosio G. Effects of tissue factor induced by oxygen free radicals on coronary flow during reperfusion. *Nat Med* 1996; **2**: 35–40.

27 Chong AJ, Pohlman TH, Hampton CR, Shimamoto A, Mackman N, Verrier ED. Tissue factor and thrombin mediate myocardial ischemia-reperfusion injury. *Ann Thorac Surg* 2003; **75**: S649–55.

28 Huang ZF, Higuchi D, Lasky N, Broze Jr GJ. Tissue factor pathway inhibitor gene disruption produces intrauterine lethality in mice. *Blood* 1997; **90**: 944–51.

29 Kamp P-B, Strathmann A, Ragg H. Heparin cofactor II, antithrombin-[beta] and their complexes with thrombin in human tissues. *Thromb Res* 2001; **101**: 483.

30 Lyon M, Deakin JA, Gallagher JT. Liver heparan sulfate structure. A novel molecular design. *J Biol Chem* 1994; **269**: 11208–15.

Haemophilia (2006), 12, 172–178 DOI: 10.1111/j.1365-2516.2006.01206.x

CASE REPORT

A case of coagulation factor V deficiency caused by compound heterozygous mutations in the factor V gene

N. YAMAKAGE,* M. IKEJIRI,* K. OKUMURA,* A. TAKAGI,*† T. MURATE,*† T. MATUSHITA,‡ T. NAOE,‡ K. YAMAMOTO,§ J. TAKAMATSU,§ T. YAMAZAKI,¶ M. HAMAGUCHI¶ and T. KOJIMA*†
**Department of Pathophysiological Laboratory Sciences, Nagoya University Graduate School of Medicine; †Department of Medical Technology, Nagoya University School of Health Sciences; ‡Department of Hematology, Nagoya University Graduate School of Medicine; §Division of Transfusion Medicine, Nagoya University Hospital; and ¶Department of Hemostatis and Thrombosis Clinical Research Center, National Hospital Organisation, Nagoya Medical Center, Nagoya, Japan*

Summary. We investigated the molecular basis of a severe factor V (FV) deficiency in a Japanese female, and identified two distinct mutations in the FV gene, a novel cytosine insertion (1943insC) and a previously reported point mutation (A5279G). We expected the patient to be a compound heterozygote for those mutations, as a 1943insC, but not an A5279G, was found in the mother and a sibling. The 1943insC will cause a frame-shift after ^{590}Gln, resulting in amino acid substitutions with two abnormal residues followed by a stop codon in the FV A2 domain (FS592X). The A5279G will cause an amino acid alteration in the FV A3 domain (Y1702C), which has been observed in several ethnic groups. We found that both mutant mRNAs were detected by reverse transcriptase polymerase chain reaction (RT-PCR) in the patient's platelets, whereas no FV antigen and activity were detected in plasma. On the one hand, the RT-PCR signal from the FS592X-FV mutant mRNA was markedly reduced, suggesting that the RNA surveillance system would eliminate most of the abnormal FS592X-FV transcripts with a premature termination. On the other hand, expression analyses revealed that only small amounts of Y1702C-FV with a low specific activity were secreted, and that the FS592X-FV was not detected in cultured media. These data indicated that both mutant FV molecules would be impaired, at least in part, during the post-transcriptional process of protein synthesis and/or in secretion. Taken together, it seems to suggest that each gene mutation could be separately responsible for severe FV deficiency, while this phenotype is due to the in-trans combination of the two defects.

Keywords: compound heterozygote, expression study, factor V deficiency, gene mutation, parahaemophilia, reverse transcriptase polymerase chain reaction

Introduction

Human coagulation factor V (FV) is a large (molecular weight of 330 kDa) single-chain glycoprotein that circulates in blood as an inactive procoagulant cofactor and plays an important role in the blood coagulation cascade [1,2]. The cDNA clones encoding human FV have been isolated [3], and the human FV gene has been mapped to chromosome 1q23 and spans approximately 80 kb of DNA [4]. The human FV gene consists of 25 exons and 24 introns, and the mRNA encodes 2224-amino acid protein containing a leader peptide of 28 amino acids [5]. It is comprised of three homologous A-type domains, two homologous C-type domains, and a heavily glycosylated B domain and shows a linear domain structure (A1-A2-B-A3-C1-C2) homologous to factor VIII (FVIII) with 35–40% homology existing in both the A-type and C-type domains [1,2]. Thrombin activates FV by the proteolytic release of the B domain, resulting in the formation of a non-covalently bound heterodimeric molecule of the heavy chain (residues 1–709, A1-A2 domains) and

Correspondence: Tetsuhito Kojima, MD, PhD, Professor, Department of Pathophysiological Laboratory Sciences, Nagoya University Graduate School of Medicine, 1-1-20 Daiko-Minami, Higashi-ku, Nagoya 461-8673, Japan.
Tel.: 81 52 719 3153; fax: 81 52 719 3153;
e-mail: kojima@met.nagoya-u.ac.jp

Accepted after revision 7 December 2005

light chain (residues 1546–2196, A3-C1-C2 domains), activated FV (FVa) [6].

Activated FV functions as an essential molecule of the prothrombinase complex that catalyses the conversion of prothrombin to thrombin by factor Xa in the presence of calcium and a phospholipid membrane. The procoagulant function of FVa is down-regulated by the anticoagulant serine protease, an activated protein C (APC) [7] that cleaves to FVa at Arg306, Arg506 and Arg679, resulting in a loss of FVa activity. On the other hand, FV cleaved by APC before thrombin activation, FVac, shows an anticoagulant function as a cofactor in the APC-mediated inactivation of activated FVIII (FVIIIa). Thus, FV plays an important role in the procoagulant pathway as well as in the protein C anticoagulant pathway [8].

Around 75% of FV in blood is in the plasma, with the residual FV in the α-granules of blood platelets. In plasma, FV exists in two isoforms (FV1 and FV2) that have different molecular weights because of partial N-linked glycosylation in the C2 domain [9]. FV1 and FV2 have different characteristics in terms of procoagulant activity, inactivation by APC, and their anticoagulant function in the protein C pathway [10]. Consequently, FV1 has the overall potential to generate more thrombin than FV2.

Factor V deficiency, also known as parahaemophilia, was first described in 1947 by Owren [11]. It is a rare bleeding disorder inherited in an autosomal recessive manner with an incidence of about one in 1 million [1]. Bleeding symptoms in FV-deficient patients are varied; heterozygotes are usually asymptomatic, whereas homozygotes may show a mild, moderate or severe bleeding tendency.

To date, more than 40 identified cases of mutations in the FV gene were described in FV-deficient patients in the homozygous or compound heterozygous state [12]. In this study, we investigated the molecular basis of severe FV deficiency in a Japanese patient, and demonstrated that she was another compound heterozygote for FV gene mutations resulting in the post-transcriptional impairment of FV synthesis and/or secretion.

Materials and methods

Preparation of plasma, genomic DNA and total RNA of platelets

Ethical approval for the study was obtained from the Ethics Committee of the Nagoya University School of Medicine. Following informed consent, blood samples from the patient, family members and volunteers were collected in a 1:10 volume of 3.13% sodium citrate. Plasma was separated by centrifugation at 2000 *g* for 20 min, and aliquots were stored at −70°C until use. The patient had not received substitution therapy for 3 months prior to blood sampling for FV antigen and activity measurements. Genomic DNA was isolated from peripheral blood leucocytes as described previously [13]. Citrated blood samples from the patient and her sibling were centrifuged at 250 *g* for 5 min at 4°C to collect platelet-rich plasma. Subsequently, the total RNA was extracted from platelets by RNA STAT-60 (Tel-Test Inc., Friendswood, TX, USA), and subjected to a reverse transcription (RT) reaction as described below.

FV antigen and activity assays

Factor V procoagulant activity and FV antigen in plasma as well as in culture media containing recombinant FV proteins were measured as described below. FV procoagulant activity was measured by one-stage clotting assay, of which the sensitivity limit and the normal range are 3% and 70–135%, respectively, using human FV-deficient plasma (George King Bio-Medical, Overland, KS, USA) and Simplastin (Biomerieux, Inc., Durham, NC, USA). FV antigen was measured by enzyme-linked immunosorbent assay (ELISA), of which the sensitivity limit and the normal range are 1% and 70–135%, respectively, using an affinity-purified sheep anti-human FV IgG as a coating antibody with a peroxidase-conjugated sheep anti-FV antibody as a second antibody, according to the manufacturer's protocol (Cedarlane Lab. Ltd, Hornby, ON, Canada). In both assays, FV levels were expressed as a percentage of control plasma pooled from 25 healthy individuals.

PCR and DNA sequencing

The polymerase chain reaction (PCR) primers were synthesized to amplify all exons and splicing junctions of the FV gene, based on the reported genomic DNA sequence of human FV (GenBank Z99572). Information of the primer sequences is available from the authors. PCR amplification of the FV gene was performed with rTaq polymerase or exTaq polymerase (Takara Bio Inc., Kusatsu, Japan) in 30–35 cycles under the following conditions: 30 s denaturing at 94°C, 30 s annealing at 47–58°C and 30 s extension at 72°C.

Polymerase chain reaction products were separated by agarose gel electrophoresis, and authentic fragments were collected and purified with a QUAEX II kit (Qiagen K.K., Tokyo, Japan). The samples were then directly sequenced by a Big Dye Terminator

Cycle Sequencing FS Ready Reaction kit (Applied Biosystems, Foster City, CA, USA) using forward or reverse PCR primers, according to the manufacturer's protocol. The sequencing products were then precipitated with 0.15 M NaOAc (pH 8.0) and cold ethanol, washed once with 70% ethanol, dried, resuspended in 25 μL of Template Suspension Reagent (Applied Biosystems), and analysed by an ABI Prism 310 Genetic Analyzer (Applied Biosystems).

Analysis of FV mRNA

To investigate the presence of FV transcripts from the mutant allele in platelets, we analysed platelet RNAs from the proband by mRNA-based PCR-restriction fragment length polymorphisms (RFLPs). In brief, total RNA extracted from the platelets was reverse-transcribed using the respective gene-specific primers: 12GSP (5′-TCTGTTCTGGTAATCA TAGT-3′) for 1943insC or 15GSP (5′-GTGCTG TTTATTGCCATTTT-3′) for A5279G, and Super Script II RT reverse transcriptase (Invitrogen Japan, Tokyo, Japan). To detect the 1943insC mutation, a nested PCR was performed using the following primers: 12rPCR-UP (5′-CCCTATAGCATTTAC CCTCA-3′) and 12GPS for the first PCR, and 12mut-UP (5′-ACTTCTGTAGTGTGGGGggCC-3′; bold lower case characters are mismatched nucleotides) and 12 M-LW (5′-TTCATCATCATCTGGG-ATAC-3′) for the second PCR, introducing a new *Apa*I restriction site in the mutant PCR products, as a single PCR using the first or second PCR primer set failed to amplify authentic PCR products. The 1943insC mutant RT-PCR products would yield 19- and 221-bp fragments, whereas the wild-type products would not be digested (239 bp). To detect the A5279G mutation, PCR was performed with the following primers: 15 M-UP (5′-AAAAATCATCA GAGGGAAAG-3′) and 15mut-LW (5′-CTGGGT TCACAGCTGAcTAG-3′) introducing a *Spe*I restriction site in the wild-type PCR products. Thus, the wild-type RT-PCR products would yield 18- and 159-bp fragments, while the A5279G mutant products would not be digested (177 bp). These fragments were run on a 4% agarose gel and stained with ethidium bromide. We evaluated the allele-specific mRNA levels by the quantitative densitometric analyses using the NIH image software (version 1.62) (National Institutes of Health, Bethesda, MD, USA).

Preparation of mutant FV expression vectors

We prepared individual FV expression vectors bearing the identified mutations, 1943insC (FS592X; the initial Met residue is denoted amino acid +1) and A5279G (Y1702C), based on pMT2 containing a full-length cDNA of human FV (pMT2-FV). Both mutations were introduced individually into the pMT2-FV expression vector using the recombinant PCR method described elsewhere [14]. After recombinant PCRs, each DNA fragment encoding the 1943insC or A5279G mutation was isolated as *Bsp*36I-*Bsp*EI or *Bsp*MI-*Sna*BI fragments, and separately replaced into the appropriate position for the pMT2/FV expression vector. DNA sequencing confirmed that no unexpected mutation was found in any of the whole mutant inserts in either construct.

Transient expression of recombinant FVs in COS-1 cells

African green monkey kidney COS-1 cells were cultured in a 5% CO_2 humidified atmosphere at 37°C in Dulbecco modified Eagle medium (DMEM; Invitrogen) supplemented with fetal calf serum (10%), glutamine (1%), and antibiotics (penicillin and streptomycin, 100 IU mL^{-1} and 100 μg mL^{-1} respectively). Cells in 30-mm dishes were transfected with either wild type or individual mutant plasmids using the Fu-GENE6™ transfection reagent (Roche Diagnostics K.K., Tokyo, Japan) according to the manufacturer's instructions. After 48-h culture of the transfected cells in serum-free DMEM, conditioned media containing the secreted recombinant proteins were collected, then concentrated using Centrisart I (cut off MW 20000; Sartorius, Goettingen, Germany), and subjected to one-stage clotting assay as well as ELISA (Cedarlane Lab. Ltd) for recombinant FV antigen measurements as described above.

Results and discussion

Case report

The patient (individual II-1, Fig. 1) is a 39-year-old Japanese woman who had recurrent episodes of bleeding such as epistaxis, joint region haematoma and hypermenorrhea, which were treated with FV replacement therapy by transfusion of fresh frozen plasma. When the patient was 4 years old, she had been diagnosed as having coagulation FV deficiency, since laboratory tests revealed that the prothrombin time and the activated partial thromboplastin time were prolonged, and FV activity was below the measurable limit. There was no history of bleeding tendencies in her other family members tested, since FV activities in plasma of both her mother and a sibling were 65%, suggesting that they might be

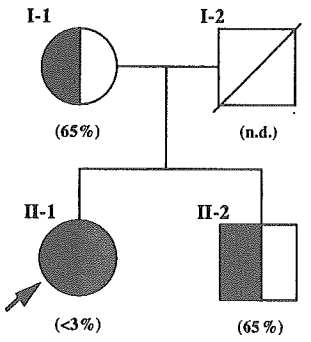

Fig. 1. Pedigree of the factor V-deficient family. The propositus is subject II-1 (arrow). Circle and square indicates male and female respectively. Values in parentheses represent plasma factor V activities (n.d., not done). Subjects with 1943insC and A5279G mutations are demonstrated with solid and shaded areas respectively.

heterozygous for FV-deficiency causing mutation. Consanguinity in the family was excluded.

DNA sequencing

In order to identify causative FV gene mutation(s) in such an FV-deficient patient, we analysed nucleotide sequences of all 25 exons and exon–intron boundaries of the FV gene. Results from direct sequencing of the FV gene revealed that the patient had a C insertion in three consecutive cytosine nucleotides [^{589}Thr(ACC)–^{590}Gln(CAG)] in exon 12 at nucleotide positions 1940–1942 (1943insC), and an A–G transition in exon 15 at nucleotide position 5279 (A5279G) (Fig. 2). DNA samples from her mother and brother also showed heterozygosity for the 1943insC mutation, but no A5279G mutation (data not shown), which are consistent with the data of plasma FV activity, i.e. about half that of normal subjects; 1943insC is a novel mutation, which can cause a frame-shift resulting in a substitution of the amino acids after ^{590}Gln with two abnormal residues (^{590}Pro–^{591}Glu) followed by a stop codon (FS592X). The A5279G will cause the amino acid substitution Y1702C, which was previously designated FV Seoul 2 [15]. The A5279G FV gene mutation has also been found in Italian and Slovenian subjects [16,17], and is thought to be a very ancient and/or recurrent mutation. In this study, we demonstrated that this mutation also occurred in a Japanese subject, suggesting that the A5279G might be a hot-spot mutation rather than a founder mutation.

mRNA analysis (RT-PCR RFLPs)

We analysed the expression of mutant FV gene transcripts from the patient's platelets by mRNA-mediated PCR-RFLPs (RT-PCR RFLPs). For 1943insC (FS592X-FV mRNA), the nested RT-PCR followed by *Apa*I digestion yielded 239- and 221-bp bands, representing transcripts from the normal and mutant alleles, respectively, although the mutant signal was markedly reduced (Fig. 3a). For A5279G (Y1702C-FV mRNA), the RT-PCR products digested with *Spe*I yielded 159- and 177-bp bands, representing transcripts from the normal and mutant alleles respectively (Fig. 3b). Thus, both mutant transcripts were present in the patient's platelets. However, the FS592X-FV mRNA signal was markedly reduced to 12% of the wild type in the quantitative densitometric analysis, whereas the Y1702C-FV mRNA signal was more intense (250% of the wild type). These data suggest that the patient could be compound heterozygous for these mutations, and that her RNA surveillance system would eliminate most of the FV mRNA derived from the mutant allele encoding a premature termination by the frame-shift mutation, FS592X [18]. On the other

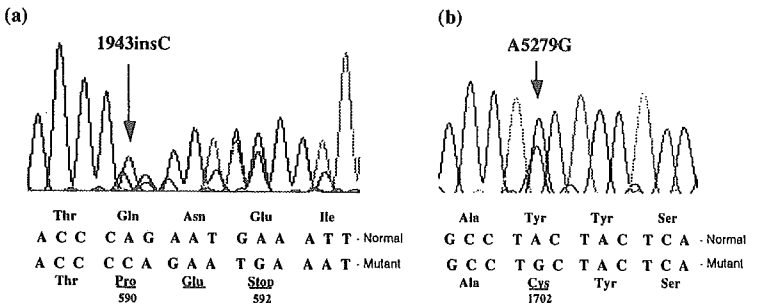

Fig. 2. Patient's nucleotide and amino acid sequences surrounding the mutations. (a) Nucleotide and amino acid sequences surrounding 1943insC. Arrow indicates mutation point. The mutation predicts an abnormal sequence of two amino acid residues and a stop codon. (b) Nucleotide and amino acid sequences surrounding A5279G. Arrow denotes mutation point. Patient's heterozygous sequencing pattern is shown.

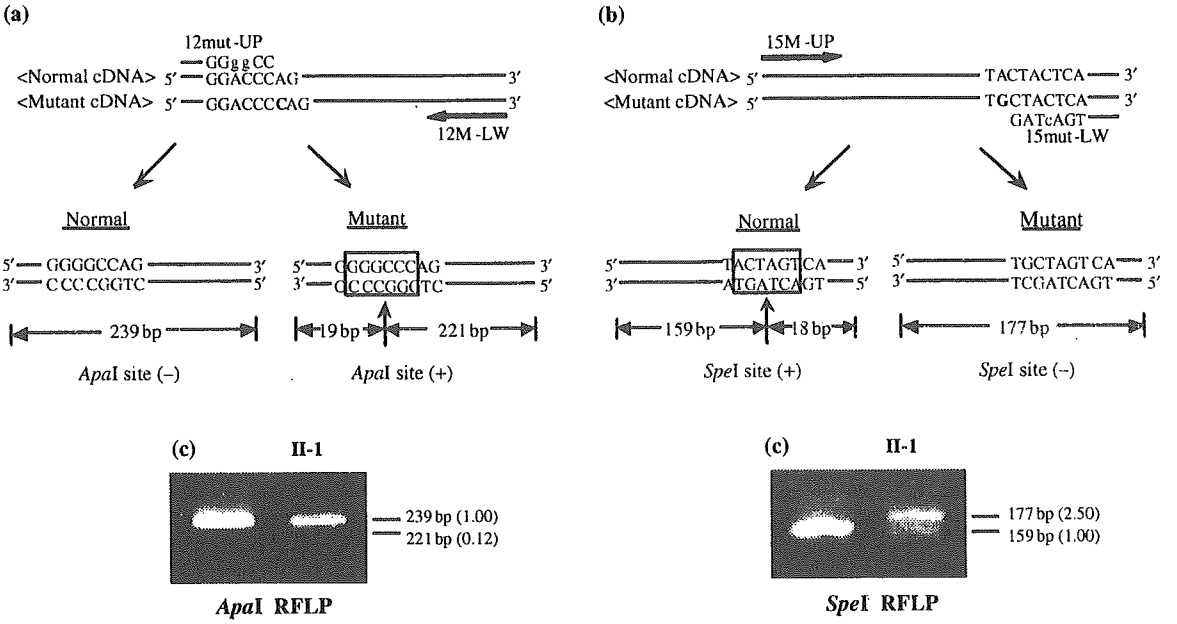

Fig. 3. Detection of mutant factor V mRNAs in patient's platelets. (a) Reverse transcriptase polymerase chain reaction (RT-PCR) products (239 bp) using primers 12mut-UP and 12M-LW were digested with *Apa*I, then electrophoresed on 4% NuSieve 3:1 agarose gel. Wild-type RT-PCR product migrated as an uncleaved 239-bp band, while FS592X (1943insC') RT-PCR product is represented by an *Apa*I cleaved 221-bp band. II-1, proband; C, control donor. Numbers in parentheses are relative amounts of signals measured by the quantitative densitometric analysis (wild type = 1.00). (b) RT-PCR products (177 bp) using primers 15M-UP and 15mut-LW were digested with *Spe*I, then electrophoresed on 4% NuSieve 3:1 agarose gel. Wild-type RT-PCR product migrated as *Spe*I cleaved 159-bp band, whereas Y1702C (A5279G) RT-PCR product is represented by an uncleaved 177-bp band. II-1, proband; C, control donor. Numbers in parentheses are relative amounts of signals measured by the quantitative densitometric analysis (wild type = 1.00).

hand, both the FV antigen and activity in her plasma were below the detectable limit, suggesting that the mutant Y1702C-FV might be impaired during the post-transcriptional process of protein synthesis and/or in secretion. Indeed, it has also been previously reported that the FV allele bearing the Y1702C mutation was expressed normally at the mRNA level, but not at the protein level in plasma [15].

Expression of wild type and mutant recombinant FVs in COS-1 cells

It is important to determine the patient's phenotype on Met1736Val polymorphism, as it will exert a great influence on the expression level of the recombinant FV [19]. Sequence analysis revealed that the patient was homozygous for 1736Met, which is the same phenotype encoded in the pMT2-FV, and thus its influence may not be revealed in expression experiments for her Y1702C-FV.

We investigated the effects of the identified mutants on FV secretion by conducting transient transfection experiments in COS-1 cells, which do not express endogenous FV. We observed that the wild type recombinant FV proteins were secreted efficiently into culture media with an adequate specific activity (0.94), but that the mutant Y1702C-FV showed an impaired secretion (1.8% of the wild type) and inadequate FV procoagulant activity (0.56) (Fig. 4). These data tend to support the conclusion that the Y1702C mutation could be causative for the FV deficiency as reported previously [15]. Indeed, plasma levels of FV activity in her mother and brother, who had only the Y1702C mutation in heterozygous, were reduced to 65% of normal. The 1702Y is a highly conserved amino acid not only in FV molecules among various species, but also in human FVIII and ceruloplasmin [15]. Moreover, an X-ray crystal structure analysis of wild type FV has demonstrated that the FV Y1702C mutation leads to the disappearance of two hydrogen bonds with P1618, and that its structure was significantly altered by a new hydrogen bond bridge formed between this cysteine and one of the other free cysteines [15]. These data suggest that 1702Y may play an important role in maintaining the structure and function of the FV molecule.

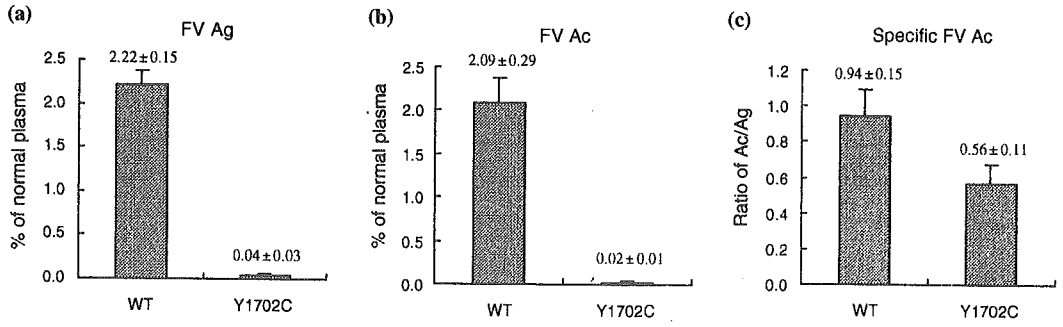

Fig. 4. Transient expression of wild-type factor V (FV) and 1702C mutant FV in COS-1 cells. Plasmids containing wild type (pMT2/FV) or mutant (pMT2/FV-Y1702C) FV cDNA were transiently transfected in COS-1 cells using FuGene reagent. Antigen and activity levels of recombinant FVs were measured in conditioned media 48 h after transfection (a, FV antigen; b, FV activity; c, FV-specific activity). Bars represent mean values ± SD of three independent experiments, each performed in duplicate. FV levels were expressed as percentage of normal pooled plasma from 25 healthy individuals.

On the other hand, recombinant FS592X-FV molecule was not detected in cultured media of the transfected COS-1 cells (data not shown). The transcripts of FS592X-FV were detected in the patient's platelets, but were found to be markedly reduced compared with normal allele transcripts (Fig. 3a). Moreover, as the FS592X-FV is a truncated molecule in the A2 domain, it would not be processed normally as reported for other mutant coagulation factors [20,21].

Conclusion

In this study, we investigated the molecular basis of a severe coagulation FV deficiency in a Japanese woman and identified two distinct mutations (1943insC/FS592X and A5279G/Y1702C) in her FV gene. The data indicated that both mutant FV molecules would be impaired, at least in part, during the post-transcriptional process of protein synthesis and/or in secretion. Taken together with the above observations, it seems to suggest that each mutation could be separately responsible for severe FV deficiency, while this phenotype is due to the in-trans combination of the two defects.

Acknowledgements

We wish to thank C. Wakamatsu for expert technical assistance. We are also indebted to M. Kyoutani, M. Yamashita, T. Yamada, and H. Okada for helpful discussions, and to Dr H. Saito (Nagoya Medical Center) for critical commentary on this paper. This study was supported in part by grants-in-aid from the Japanese Ministry of Education, Culture, Sports, Science and Technology (17590490) and the Japanese Ministry of Health, Labor and Welfare (Research on Specific Diseases).

References

1 Kane W, Davie E. Blood coagulation factors V and VIII: structural and functional similarities and their relationship to hemorrhagic and thrombotic disorders. *Blood* 1988; 71: 539–55.
2 Kane W. Factor V. In: Colman RW, Hirsh J, Marder VJ, Clowes AW, George JN, eds. *Hemostasis and Thrombosis Basic Principles and Clinical Practice*, 4th edn. Philadelphia, PA: Lippincott Williams and Wilkins, 2001; 157–69.
3 Jenny RJ, Pittman DD, Toole JJ *et al.* Complete cDNA and derived amino acid sequence of human factor V. *Proc Natl Acad Sci USA* 1987; 84: 4846–50.
4 McAlpine PJ, Coopland G, Guy C *et al.* (SPTA1) and coagulation factor V (F5). *Cytogenet Cell Genet (Abstract)* 1989; 51: 1042.
5 Cripe LD, Moore KD, Kane WH. Structure of the gene for human coagulation factor V. *Biochemistry* 1992; 31: 3777–85.
6 Suzuki K, Dahlbäk B, Stenflo J. Thrombin-catalyzed activation of human coagulation factor V. *J Biol Chem* 1982; 257: 6556–64.
7 Suzuki K, Stenflo J, Dahlbäck B, Teodorsson B. Inactivation of human coagulation factor V by activated protein C. *J Biol Chem* 1983; 258: 1914–20.
8 Thorelli E, Kaufman RJ, Dahlbäck B. Cleavage of factor V at Arg 506 by activated protein C and the expression of anticoagulant activity of factor V. *Blood* 1999; 93: 2552–8.
9 Nicolaes GAF, Villoutreix BO, Dahlbäck B. Partial glycosylation of Asn^{2181} in human factor V as a cause of molecular and functional heterogeneity. Modulation of glycosylation efficiency by mutagenesis of the consensus sequence for N-linked glycosylation. *Biochemistry* 1999; 38: 13584–91.

10 Hoekema L, Nicolaes GAF, Hemker HC, Tans G, Rosing J. Human factor Va^1 and factor Va_2: properties in the procoagulant and anticoagulant pathways. *Biochemistry* 1997; **36**: 3331–5.
11 Owren P. Parahemophilia: hemorrhagic diathesis due to absence of a previously unknown clotting factor. *Lancet* 1947; **1**: 446–8.
12 Asselta R, Tenchini ML, Duga S. Inherited defects of coagulation factor V: the hemorrhagic side. *J Thromb Haemost* 2006; **4**: 26–34.
13 Kojima T, Tanimoto M, Kamiya T *et al.* Possible absence of common polymorphisms in coagulation factor IX gene in Japanese subjects. *Blood* 1987; **69**: 349–52.
14 Higuchi R. Recombinant PCR. In: Innis MA, Gelfand DH, Sninsky JJ, White TJ, eds. *PCR Protocols: A Guide to Methods and Applications*. San Diego, CA: Academic Press, Inc., 1990: 177–83.
15 Castoldi E, Simioni P, Kalafatis M. *et al.* Combinations of 4 mutations (FV R506Q, FV H1299R, FV Y1702C, PT 20210G/A) affecting the prothrombinase complex in a thrombophilic family. *Blood* 2000; **96**: 1443–8.
16 van Wijk R, Nieuwenhuis K, van den Berg M *et al.* Five novel mutations in the gene for human blood coagulation factor V associated with type I factor V deficiency. *Blood* 2001; **98**: 358–67.
17 Montefasco MC, Duga S, Asselta R *et al.* Clinical and molecular characterization of 6 patients affected by severe deficiency of coagulation factor V: broadening of the mutational spectrum of factor V gene and in vitro analysis of the newly identified missense mutations. *Blood* 2003; **102**: 3210–6.
18 Maquat LE, Carmichael GG. Quality control of mRNA function. *Cell* 2001; **104**: 173–6.
19 Yamazaki T, Nicolaes GAF, Sorensen KW, Dahlbäck B. Molecular basis of quantitative factor V deficiency associated with factor V R2 haplotype. *Blood* 2002; **100**: 2515–21.
20 Katsumi A, Senda T, Yamashita Y *et al.* Protein C Nagoya, an elongated mutant of protein C, is retained within the endoplasmic reticulum and is associated with GRP78 and GRP94. *Blood* 1996; **87**: 4164–75.
21 Yamazaki T, Katsumi A, Kagami K *et al.* Molecular basis of a hereditary type I protein S deficiency caused by a substitution of Cys for Arg474. *Blood* 1996; **87**: 4643–50.